Spectra of Body Waves from Local Small Earthquakes in the Southern Parts of Kyoto

By Tamotsu FURUZAWA, Kojiro IRIKURA, Shuzo TAKEMOTO
and Junpei AKAMATSU

Abstract

Seismic waves from local small earthquakes occurring in the southern parts of Kyoto were observed with magnetic data recorders at the Amagase Crustal Movement Observatory, and the spectral densities of body waves were analyzed.

Magnitudes of analyzed events are in the range from 1.0 to 2.5. Peak frequencies of spectral densities seem to depend not only on magnitude but also on location of the source, that is, peak frequencies of P waves from events in the region where microearthquakes occur concentratedly, were lower than those from events in another region where seismic activity is very low. These observed results suggest that regional variation of physical properties such as strength and shear modulus exists in the crust.

1. Introduction

Okano and Hirano have shown that microearthquakes in the vicinity of Kyoto occur concentratedly in a belt-like zone lying from the west coast of Lake Biwa to Osaka Bay and have similar distributions of initial motions of P waves[1]. The observed facts that earthquakes occur in the bounded region seem to suggest that physical properties such as strength and shear modulus vary regionally in the crust. This has been also examined through the regional variation of aftershock activity.[2] As these studies are based on statistical examination, it seems that quantitative estimations of the physical properties in the crust are impossible, thus, for further discussion it would be necessary to estimate the quantities such as moment, energy and stress drop for individual earthquakes.

The examination of spectral densities of seismic waves seems to be useful for the estimation of source parameters, and this method has been mainly applied to large earthquakes at a distance. But it has been applied seldom to local small earthquakes. This may be due to the fact that since higher frequency components are predominant in the seismic waves, station correction and phase identification are difficult. Nevertheless, in order to discuss the regional variation of physical properties with dimensions of a few tens of kilometers, it may be useful to analyze spectral densities of local small

earthquakes with small source dimensions.

From these analyses the locality of the scaling law of earthquakes and its dependency on the regional difference of physical properties in the crust may be discussed. This will give an important clue for relating the occurrence of earthquakes to the observational data of crustal deformation, and for estimating possible magnitude and source mechanism in the region in question.

It sould be necessary, however, for examination of spectra of local small events, to make accurate observations with magnetic data recorders and to consider the way of analysis proper to observed seismograms.

From the above point of view we analyzed seismic waves from local small events, occurring in the southern parts of Kyoto, observed with magnetic data recorders at the Amagase Crustal Movement Observatory. The characteristics of the spectral densities are discussed in connection with source regions. The method of analysis is also discussed.

2. Observation and data preparation

Analyzed seismograms were obtained through the temporary observations at the Amagase Crustal Movement Observatory (34°52′48″ N, 135°50′09″ E), in the southern parts of Kyoto, using three components seismometers (1 Hz, 3 volts/kine), DC amplifiers and magnetic data recorders. Periods of the observations and the instrumental constants are listed in Table 1.

As apparent predominant frequencies of P waves of seismograms were less than about 20 Hz, analog high cut filters were operated before digitization to remove disturbance of phase from higher frequency noises and to avoid aliasing. The filters have cut-off frequencies at 25 Hz and an attenuation rate of 30 db/oct.

Filtered seismograms were digitized at sampling intervals of 0.01 sec by use of an A-D converter which can sample three channels without time delay between channels.

Overall instrumental response is shown in Fig. 1.

Table 1.   Periods of observations and the instrumental constants.

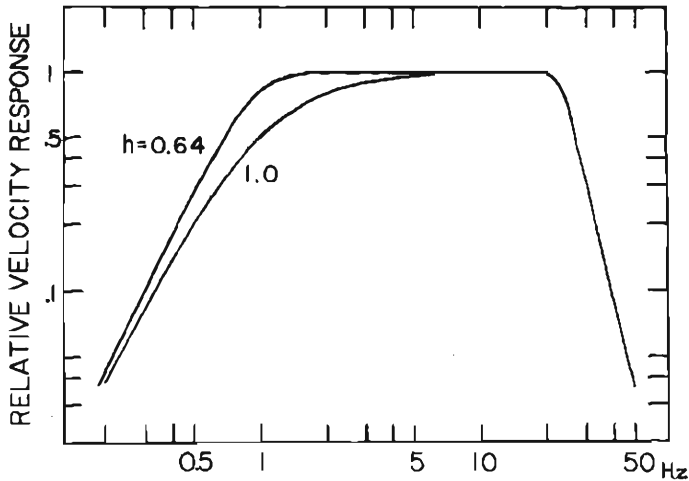| Period of observation	h of seismometers	Gain of DC amplifiers
July 13~July 19, 1969	1.0	1000
Aug. 4~Aug. 8, 1969	1.0	4000
Aug. 4~Aug. 11. 1970	1.0	500
Aug. 20~Aug. 25, 1970	1.0	500
Aug. 26~Sept. 1, 1970	1.0	1000
July 15~Aug. 16, 1971	0.64	1000

Fig. 1. The overall instrumental response curve.

3. Particle motions

Seismic waves from small near events are mainly of high frequency components, and are likely to be affected by small geological structure, lateral inhomogeneity and topography of the crust. In order to study their spectra deterministically, it is necessary to identify the phase of interest and to clarify their characteristics. This may be carried out through examination of directions and rectilinearity of particle motions.

Examples of filtered seismograms and particle motions of P and S portions are shown in Figs. 2–4. Fig. 2 shows a very near event with t_{s-p} (*S-P* time) of 1.66 sec. In the horizontal plane the linearities of both P and S waves are well, and the direction of S motions is nearly orthogonal with that of P, showing SH waves. From the direction of P motions, NS- and EW- components were converted into radial and transverse ones, and particle motions in the vertical plane were obtained. In the vertical plane the direction of S motions is also orthogonal with that of P, and this phase is considered to be SV waves with smaller amplitude than SH waves as shown in Fig. 2. Both P and S phases are found to be disturbed by another phases immediately after the initial motions. Fig. 3 and Fig. 4 show the events with t_{s-p} of 2.73 sec and 4.15 sec, respectively. Although the linearity of P initial motions is good, the linearity of the S ones is not so remarkable. As these events occurred at same depth (5–10 km), the incident angles are considered to be larger in the case of larger t_{s-p}. Linearity of particle motions of SV waves depends on incident angle, and beyond critical incident angle, particle motions are nonlinear.[3],[4] In Fig. 3 the particle motions of the portion before S waves are shown. This portion is considered to be P waves converted from S ones, from the fact that the direction of motion is nearly the same to that of P, and that the frequency resembles that of S rather than P. Identification of converted waves seems difficult by use of seismograms alone, but careful examination of particle motions
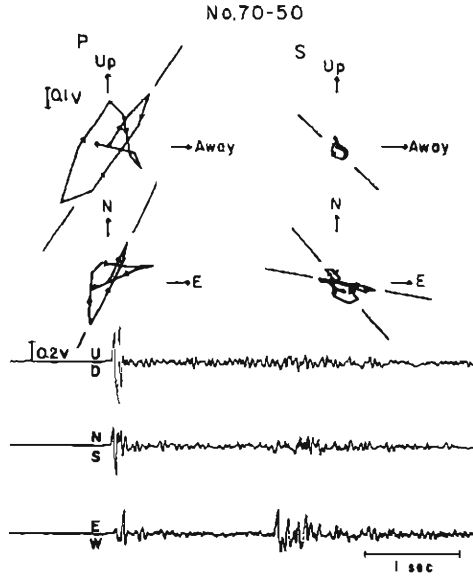
No.70-50

Fig. 2.   The 25 Hz low-pass filtered seismograms and the particle motion
           diagrams of P and S waves measured on the vertical and the
           horizontal planes of the event with t_{s-p} of 1.66 sec.

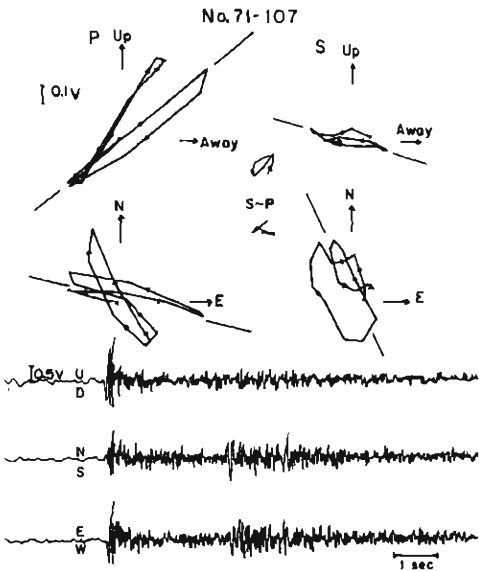No. 71-107

No.70-120

Fig. 3.   The 25 Hz low-pass filtered seismograms
           and the particle motion diagrams of
           P,S-converted-P and S waves of the event
           with t_{s-p} of 2.73 sec.
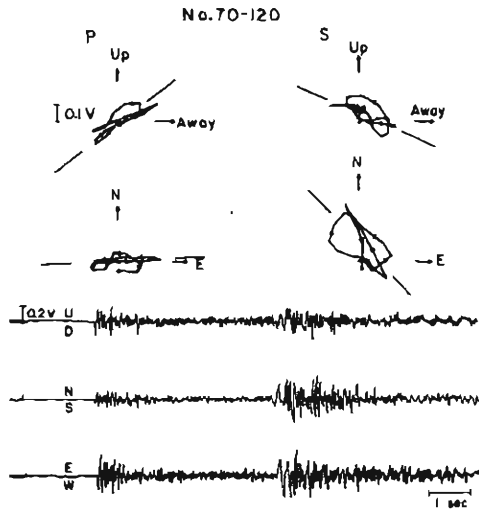
Fig. 4.   The 25 Hz low-pass filtered seismograms
           and the particle motion diagrams of P
           and S waves of the event with t_{s-p} of
           4.15 sec.

may make it possible.

In so far as the events with t_{s-p} of less than 5 sec, although both P and S waves begin to be disturbed after about 0.1 sec from the initial motions, particle motions are considered to show the characteristics of body waves from their linearity and orthogonality. From the above considerations we may conclude that initial motions of P and S waves may be examined through spectral densities in the frequency range up to 25 Hz.

4. Analysis of velocity spectra of body waves

As described in the previous section, initial portions of P and S waves show the characteristics of body waves. Examination of spectra of these portions was intended.

The interval of analysis for spectra should be selected according to the objects; to obtain the data about the velocity structure beneath the observational point, with assumption of horizontal layering, the interval should be taken long, according to the depth of the layers, enough to contain the waves reverberated between the boundaries. On the other hand, to obtain the informations about source, it should be taken short enough not to be disturbed by interference of secondary generated waves.

In almost all of the seismograms obtained, later phases with large amplitude appear seldom within about 1.0 sec after initial motions. In the section 4–2, 0.64 sec interval, in which waves considered to travel from source with less disturbance, was used to examine spectra of P waves in connection with source. As the durations of S portions are longer with large amplitude, 1.28 sec interval is used. In the section 4–1, as we intend to consider the site condition, 1.28 sec interval for P waves were used.

Fourier transformation was carried out through the Cooley and Turkey method. To remove the effect of truncation, the Hamming-Turkey formula was applied. Finally the spectral densities of particle velosities were obtained after the correction of the instrumental response in the frequency range from 0.5 to 25 Hz. 61 local small events with t_{s-p} less than 5 sec were analysed, and are listed in Table 2.

4.1 Effects of the site condition on spectra and its reduction

The effects of the plane free surface on plane P waves observed at the surface depend only on incident angle as is well known. But they depend not only on incident angle but on frequency and depth, when observed at depth, because of the interference of incident waves and reflected ones from the free surface. The velocity of P wave is 4.6–4.7 km/sec to the depth of at least 700 m near the station.[5] Theoretical spectra of the observational site at depth of 140 m are calcurated by means of the Thomson-Haskell matrix method with a half space model of $V_p = 4.66$ km/sec, $V_s = 2.45$ km/sec and $\rho = 2.5$ gr/cm^3 as shown in Fig. 5. The response of the vertical component is characterized by a large trough around 8 Hz independent of the incident angle. In the case of radial one, however, the trough varies between 3 and 6 Hz depending on the incident angle. Though observed spectra depend additionally both on the source and the propagation path, effects of site condition may be examined through a spectral

Table 2. List of the analyzed local small earthquakes. The sense, direction and incident angle of initial motion were determined by use of particle motion diagram. The types of spectra are shown in Fig. 8.

Earthquake No.	Date	s-p time (sec.)	Direction of P wave	Apparent incident angle of P wave	Initial motion P	Initial motion SH	Azimuth of epicenter	Magnitude	Type of spectra
71–073	7.25 '71	2.70	127		−	−			
69–192	8.15 '69	2.21	123	58	−				C
71–163	8. 7 '71	2.20	109		−		99		C
71–208	8.12 '71	2.28	96	35	−				B
69–002	7.13 '69	1.87	33	56	+	−	43		B
69–229	8.16 '69	1.86	32	40.5	+	+			D
69–259	8.18 '69	1.85	31		+				A
71–138	8. 4 '71	1.39	54		+		40	1.3	
70–045	8.23 '70	2.42	41	56	+	+	40	2.0	C
69–030	8. 7 '69	2.80	31	49	+	+	20		D
71–082	7.27 '71	1.32	48		+		19		BC
69–261	8.18 '69	1.75	25	41.5	+	+			D
69–045	8. 8 '69	1.75	25	43	+	+	12		A
69–213	8.16 '69	2.53	15	52.5	+	+			B
69–228	8.16 '69	3.65	−13	47	+	+			B
71–124	8. 1 '71	(4.9)	−14		+		−11		
71–193	8.11 '71	3.22	−20		+		−19		D
71–119	7.31 '71	3.24	−30		+		−23	1.7	AD
69–253	8.17 '69	3.64	−25	40	+	+	−25		A
69–067	8.10 '69	2.33	−35	35	−	−			A
70–055	8.25 '70	3.67	−43	39	+	−	−34		AB
69–011	7.19 '69	3.38	−44	41.5	+	−			B
71–096	7.28 '71	3.49	−46		+		−38	2.1	BC
70–098	8.30 '70	2.62	−57	41	+	−	−40		BC
70–078	8.27 '70	2.64	−42	39	+	−	−42	1.5	D
70–103	8.30 '70	2.18	−45	40	+	−	−42		BC
69–087	8.12 '69	3.14	−55	47.5	+	±			A
70–053	8.25 '70	3.16	−60	51	−	−	−48	2.5	AB
70–054	8.25 '70	3.17	−61	51	−	−	−48	2.4	A
71–243	8.15 '71	(2.40)			−				
71–149	8. 6 '71	(3.67)	−53		−		−58	1.5	
71–140	8. 4 '71	(3.67)	−82		−		−58	2.0	
71–072	7.24 '71	3.70	−61		−		−59	2.3	B
70–063	8.26 '70	2.04	−66	50	−	−	−59		C
69–178	8.14 '69	1.95	−73	46	−	+			D
70–031	8.20 '70	3.95	−82	(33)	−		−61	1.8	
71–253	8.16 '71	2.40			−		−64		B
69–009	7.19 '69	2.57	−71	47.5	−	+			D

71–036	7.20 '71	4.37	−75		—		−71	2.5	B
71–107	7.30 '71	2.73	−82		—		−73	2.4	B
69–023	8. 6 '69	4.09	−74	50	—	—	−73		B
71–121	8. 1 '71	3.02	−90	(28)	—		−73		
71–088	7.27 '71	2.67	−79		—		−75	2.2	B
71–245	8.15 '71	3.48	−80		—		−76	1.2	B
70–075	8.27 '70	4.94	−85	56	—		−78	1.6	B
70–052	8.25 '70	3.17	−83	43	—	—	−80		BC
71–048	7.21 '71	4.86	−81		—		−81	2.4	B
71–234	8.13 '71	4.31	−84	35	—		−90		A
70–120	9. 1 '70	4.15	−93		—		−92	2.2	B
70–074	8.27 '70	3.97	−87	54	—	—	−92		
71–206	8.12 '71	4.24	−87	47.5			(−92)	1.0	D
71–232	8.13 '71	4.10	−89	45	—		−93	2.0	BC
70–116	9.01 '70	4.15	−86		—	—	−93	2.2	B
71–115	7.31 '71	4.15	−93		(−)		−93		
71–227	8.13 '71	3.96	−99	(42)	—		−94		D
70–109	8.31 '70	3.75	−118	61	—	+	−122		B
70–118	9. 1 '70	1.38	−132	43	—	+	−136	1.8	C
69–034	8. 8 '69	3.44	−136	49	+	—	−135		C
71–152	8. 7 '71	1.38	−142		—				
70–050	8.24 '70	1.66	−154	34	+	—	−160	1.6	C
69–078	8.11 '69	2.72	−180	41	+	+			C

ratio of of vertical component to radial one. Three examples of observed spectral ratios and calculated ones of the half-space model are shown in Fig. 6. Apparent incident angles of these events are determined to be in the range of 34°–50° from the directions of the particle motions. In the frequency range lower than 17–18 Hz, the observed ratios agree well with the calculated ones and are considered to show the interference of the fundamental order. In the range above 20 Hz, however, interference of the higher order is not seen in the observed spectral ratios; it may be interpreted from that in the higher frequency range effects of attenuation and dissipation may be larger.

The periods of 2–5 Hz width of relatively small peaks and troughs in the observed spectral ratios are considered to reflect the velocity structure. The layer with P wave's velocity of 5.5 km/sec, determined by the Research Group for Explosion Seismology, may exist below the surface layer with a velocity of 4.6–4.7 km/sec. But the effect of interference due to the boundary between these two layers may be not so large as that due to the free surface because of the small contrast between velocities.

It seems unreasonable to remove the effects of the fine structure under the assumption of horizontal layering from the observed spectra, since the existance of lateral inhomogeneity of the crust should be taken into consideration. For the station correction, therefore, we proposed to reduce peaks and troughs with the periods of 2–5 Hz width through smoothing the spectra. Smoothing is carried out by taking the mean
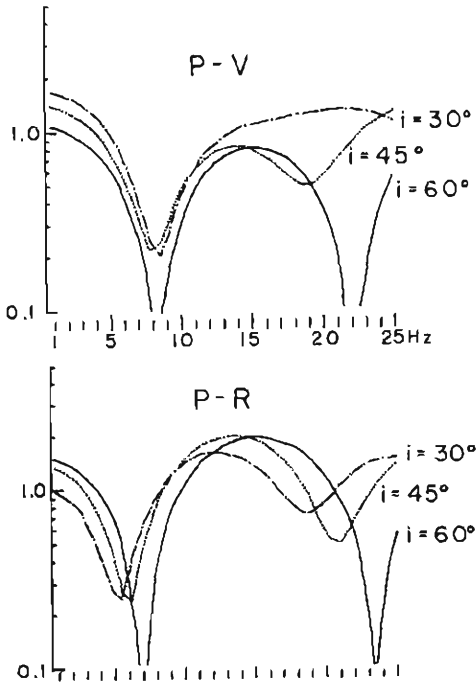
Fig. 5. Vertical and radial components of transfer
         functions for P waves.   Half-space
         parameters are; $V_p = 4.66$ km/sec, $V_s = 2.45$ km/sec, $\rho = 2.5$ gr/cm³ and the depth
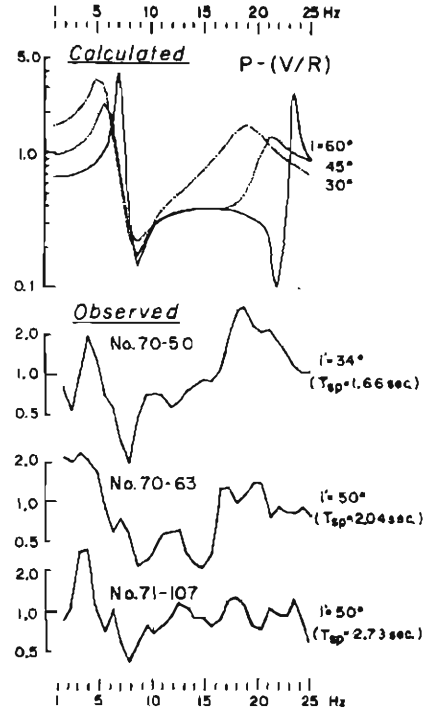   of observational point $= 140$ m.

Fig. 6. Theoretical and observed spectral ratios
         of P waves.   The parameters of the
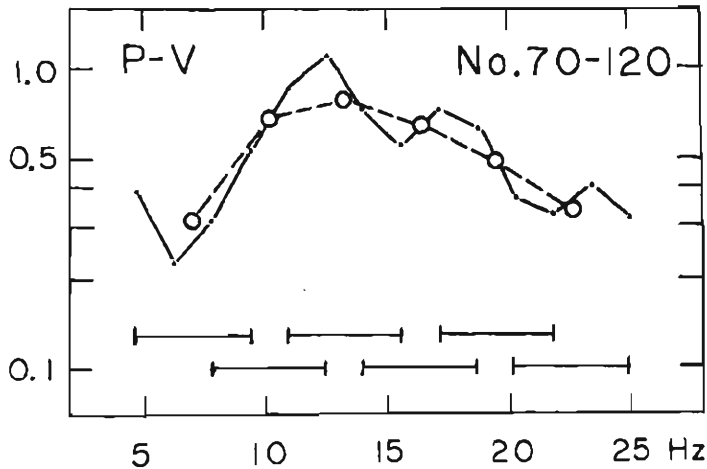   model are the same as those in Fig. 5.

Fig. 7. Smoothed spectrum and the original one of vertical component
         of P waves.   Subranges for taking the mean are also shown.

of the spectra in the subrange of 6 Hz width shown in Fig. 7. And also smoothed spectrum is compared with the original one in Fig. 7. Although this smoothing may not reduce the effects of the fundamental order's interference due to the free surface, it may be sufficient for the station correction in order to examine the variation of spectra of body waves by means of relative comparison among their figures. Because the interference of the fundamental order does not depend on the incident angle in the vertical component of P waves as shown in Fig. 5.

4.2 Regional variation of smoothed spectra

As the effects of the site condition are weakened in the smoothed spectra as is discussed in the section 4–1, the shape of the spectra of the vertical component may be discussed in connection with source and path.

Predominant frequency of spectra is considered to be a measure of source size. Smoothed spectra are classified into the four groups (A, B, C and D type) on the whole based on their peak frequencies as shown in Fig. 8. The events of A type have the lowest peak frequencies ($<$10 Hz), those of B type have relatively higher ones (13–16 Hz), and those of C type have the highest ones ($>$20 Hz). The spectra of D type are almost flat without predominant peaks.

The magnitudes of these events are less than 2.5 and there is no noticeable difference of magnitude among these four groups.

In Fig. 9 the types of spectra above mentioned are plotted at the hypocenters with each symbol, and the initial *push* and *pull* motions are shown with closed and open symbols, respectively. The distribution of the type of spectra seems to be as follows;

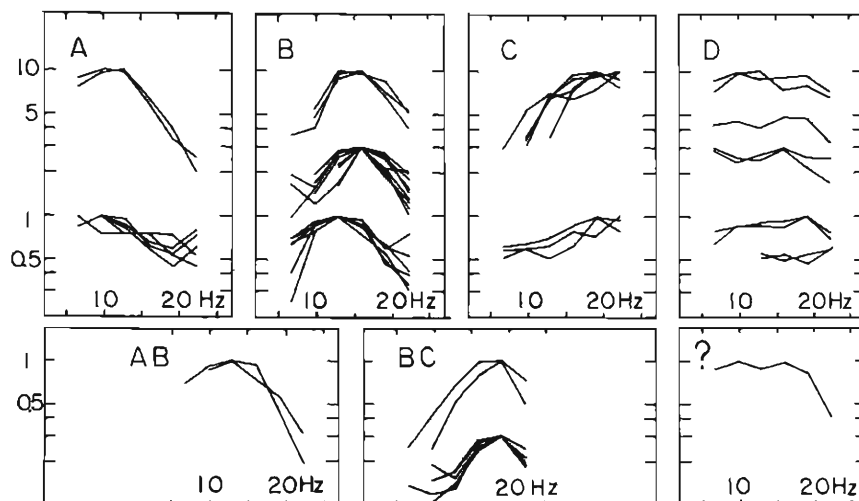(1) events of A type with initial motions of *push* occur frequently in the northern region,

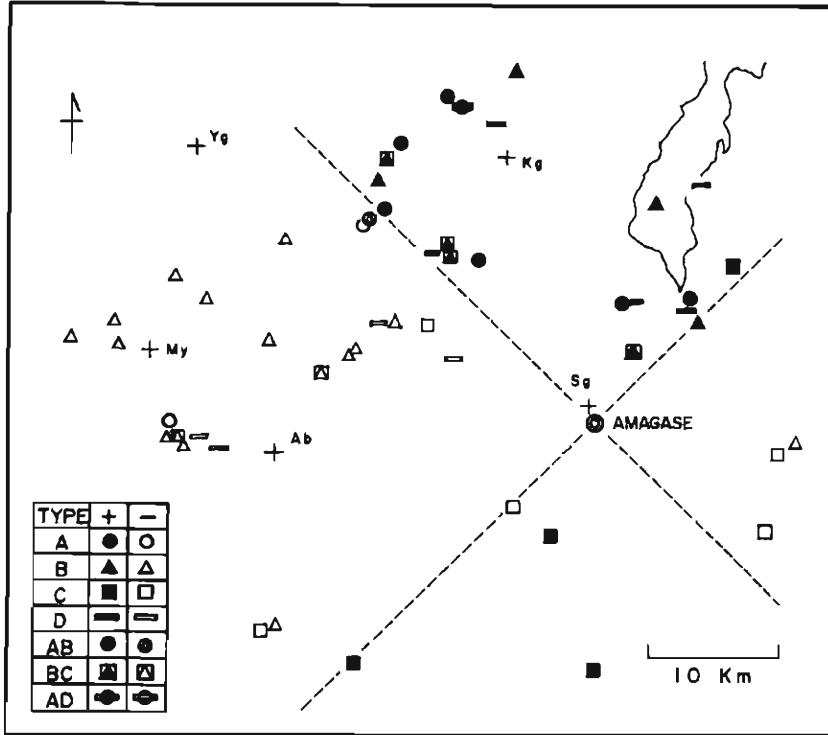Fig. 8. Smoothed spectra of P waves classified into four types, A, B, C and D.

Fig. 9. The regional variation of smoothed spectra of P waves. Type
of the spectra are shown in Fig. 8. Closed and open symbols
denote *push* and *pull* initial motions, respectively.

(2) events of B type with initial motions of *pull* occur frequently in the region
between northwest and west,

(3) events of C type with initial motions of both *push* and *pull* occur in the
southern region away from the active region called Yodo River seismically active zone,

(4) there are relatively narrow regions where events of various types occur, such
as in the directions of north-northeast and west.

In Fig. 10 are shown the smoothed spectra of transverse component of S waves;
all events in the left figure are A type classified from P waves, and those in the right
ones are C type. Even from the same group, the spectral shapes of S waves are rather
different individually. As shown in Fig. 11, however, the mean spectra obtained
from all events belonging to each group classified from P waves have the similar ten-
dency of peak frequencies as that of P waves.

5. Discussion

Observed spectra $U(\omega)$ may be expressed in terms of source spectra $S(\omega)$ and
effects of propagation path $P(\omega)$. If $P(\omega)$ is assumed to be presented by effective Q
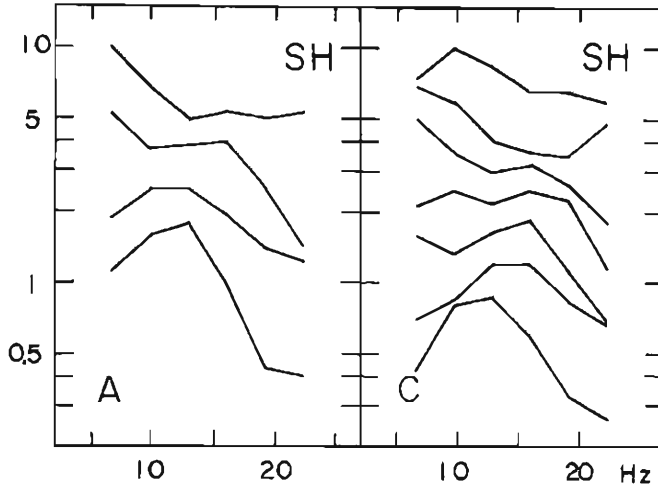value,

Fig. 10. Smoothed spectra of SH waves of the events whose spectra of P waves are A type (left) and C type (right), respectively.
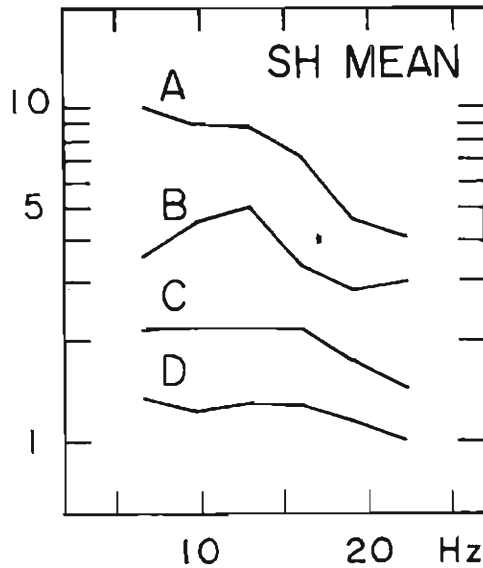

Fig. 11. Mean spectra of SH waves of the events classified by P waves' spectra.

$$U(\omega)=S(\omega)\cdot P(\omega)=S(\omega)\cdot\frac{1}{r}\cdot\exp\left(-\frac{\omega r}{2Qv}\right),\tag{1}$$

where r is length of path and v is propagation velocity. The logarithm of spectral ratio of different frequency components is

$$\ln\frac{U(\omega_1)}{U(\omega_2)}=\ln\frac{S(\omega_1)}{S(\omega_2)}-\frac{\omega_1-\omega_2}{2Qv}\cdot r,\tag{2}$$

where Q value is assumed constant in the frequency range concerned. The relations of the ratio to t_{s-p} are shown in Fig. 12 for two groups; one consists of events with initial motions of *push* in the northern region where events of A type occur mainly, another consists of events with *pull* in the western region where events of B type occur mainly. Assuming the ratio $S(\omega_1)/S(\omega_2)$ is constant, effective Q values are estimated by the least square fit of eq. (2) as shown in Fig. 12 for the frequency range of 10–25 Hz; for the northern region $280<Q<3,100$ and for the western region $390<Q$ in the 75% confidence limit. In the Q value of the two groups a meaningful difference is not seen. Large scattering of the ratio in Fig. 12 seems rather to show that the assumption on source spectra ($S(\omega_1)/S(\omega_2)$=const.) may not be reasonable. From these results the locality of the observed spectra shown in Fig. 9 seems to be attributed to the regional variation of source spectra rather than to that of the effects of paths.

Locality of spectra of S waves is not so clear as that of P waves. This may be caused by differencies of various conditions; *e.g.* contamination of P coda, effects of
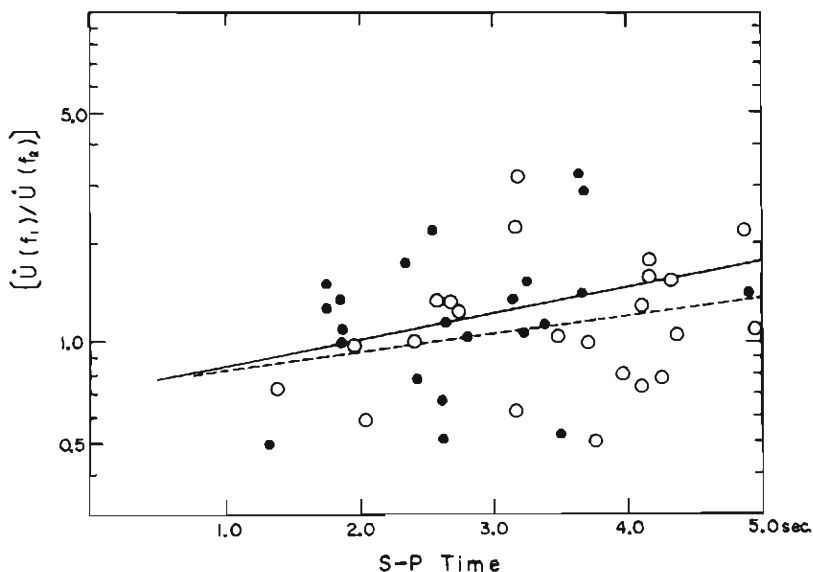

Fig. 12.   Spectral ratio of P waves.   Averaged spectral amplitudes are
used for $U(f)$; $5<f_1<15$ Hz, $15<f_2<25$ Hz.   Closed and
open circles denote *push* and *pull* initial motions, respectively.

Table 3. The trough frequencies of spectra of SH waves calcurated from a half space model. The parameters of the model are the same as those in Fig. 5. m denotes the mode number of interference and i the incident angle, respectively.

m \ i	30°	40°	50°	60°
0	5.0Hz	5.8	6.8	8.8
1	15.2	17.2	20.4	26.4

the relatively long intervals of analyses which will include undesirable later phases, and the different way of interference of the incident waves and the reflected ones from the free surface. In the case of SH waves observed underground, the interference of the fundamental order depends on the incident angle in contrast with vertical component of P waves, making a trough at 5.0–8.8 Hz as is shown in Table 3. Therefore station correction through smoothing is considered unsatisfactory. The result of the mean spectra, however, is regarded to agree with that of P waves as shown in Fig. 11.

The region where events of A and B type occur seems to correspond to the seismically active region pointed by Okano and Hirano. In the southern region where events scarcely occur, the spectra of C type are dominant. Regional variation of source spectra to be connected with seismic activity are considered interesting for estimating physical properties, such as strength and shear modulus in the crust.

Deterministic discussion about spectra of seismic waves in high frequency range is thought to have limitations because of difficulty of station correction. K. Aki treated seismic coda of small near events as back scattered surface waves which is assumed to be affected randomly by lateral inhomogeneity and topography, and intended to relate spectral density of coda to seismic moment directly.[6] In order to examine source parameters of local small earthquakes, deterministic analyses and statistical considerations such as coda analysis should be studied together.

6. Conclusion

Some conclusive remarks are obtained from discussion of the method of analysis and examination of the spectra of body waves.

(1) Examination of linearity and directivity of particle motions is useful to identify the various phases and to check the characteristics of waves as body waves (Figs. 2–4).

(2) Station correction for spectra was made with smoothing, which is available for vertical component of P waves, but is not so available for SH waves.

(3) Smoothed spectra of P waves are classified into the four groups on the whole (Fig. 8), and are considered to vary regionally (Fig. 9). Regional variation of observed spectra is regarded to be caused by that of source spectra because the attenuation of waves during propagation is considered not to depend on the difference of paths (Fig. 12).

(4)   The results of (3) suggest the regional variation of the physical properties such as strength and shear modulus in the crust.

(5)   Not only the deterministic analysis of the spectra of body waves but also statistical analysis of seismic coda should be necessary to estimate the source parameters of local small earthquakes.

References

1)   Okano, K. and I. Hirano: Earthquakes occurring in the vicinity of Kyoto. J. Phys. Earth, Vol. 16, Special Issue, 1968, pp. 141–152.

2)   Okano, K.:   Aftershock activity in the vicinity of Kyoto, Bull. Disas. Prev. Res. Inst., Kyoto Univ., Vol. 20, 1970, pp. 17–22.

3)   Nuttli, O.:   The effects of the earth's surface on the S waves particle motion, Bull. Seism. Soc. Amer., Vol. 51, 1961, pp. 237–246.

4)   Furuzawa, T. and K. Irikura: The direction of the particle motions of locall small earthquakes, Annuals of Disas. Prev. Res. Inst., Kyoto Univ., No. 13A, 1970, pp. 149–161 (in Japanese).

5)   Furuzawa, T., S. Takemoto, K. Irikura and J. Akamatsu: Local crustal effects on earthquake seismograms, Annuals of Disas. Prev. Res. Inst., Kyoto Univ., No. 14A, 1971, pp. 189–202 (in Japanese).

6)   Aki, K.:   Analysis of the seismic coda of local earthquakes as scattered waves, J. Geophys. Res., Vol. 74, No. 2, 1969, pp. 615–631.